A Mutual Coupling Model for Massive MIMO Applied to the 3GPP 3D Channel Model

Stefan Pratschner*†, Sebastian Caban*†, Stefan Schwarz*† and Markus Rupp*
*Institute of Telecommunications, TU Wien, Austria
†Christian Doppler Laboratory for Dependable Wireless Connectivity for the Society in Motion
{spratsch,scaban,sschwarz,mrupp}@nt.tuwien.ac.at

***Abstract*—Massive Multiple-Input Multiple-Output (MIMO) has become one of the key technologies for future mobile communication systems. Although there is a variety of potential benefits, unresolved implementation issues of massive MIMO are manifold. In this work, we consider the issue of mutual coupling in large antenna arrays. A known matrix model that describes array coupling effects is considered. This coupling model is augmented by a matching network in order to provide a universal coupling model that is applicable to any channel model. Impact of array coupling is then shown by applying the coupling matrix on the 3rd Generation Partnership Project 3D channel model. We show that the matching network leads to decorrelation and significantly reduces capacity losses due to mutual coupling in the context of massive MIMO.**

***Index Terms*—massive MIMO, mutual coupling, coupling model, large arrays**

I. Introduction

Multiple-Input Multiple-Output (MIMO) technologies facilitate high spectral efficiency. They are a key part of today's wireless communication standards, such as IEEE 802.11 or 3rd Generation Partnership Project (3GPP) LTE-Advanced. In the last years, MIMO systems with a large number of antennas, referred to as massive MIMO, were considered in literature [1]–[4]. When the number of antennas approaches infinity, opportunities such as asymptotically orthogonal channels and utilization of linear receivers emerge. Due to the possible enhancements in spectral efficiency and power efficiency, massive MIMO became one of the key physical layer technologies for fifth generation mobile communication networks.

Even though massive MIMO provides numerous opportunities, practical realizations still struggle with many implementation issues. Not only are theoretical limits of channel state information and pilot contamination [3]–[6], which are linked to array reciprocity calibration [7], [8], subject of ongoing research. Hardware impairments such as I/Q-imbalance, phase noise and power-amplifier non-linearities are considered in literature as well [9].

Another issue that is existing in MIMO systems is mutual coupling between antenna elements within an array [10], [11]. Mutual coupling and correlation in massive MIMO systems are investigated in [2]. However, the authors of [2] do not consider any geometric or stochastic channel model. They generate identically and independently distributed channel coefficients and introduce correlation via the Kronecker model.

Contribution: In this work, we employ a known generic matrix coupling model. This allows to introduce effects of mutual coupling to a channel matrix that might be obtained by any channel model. In contrast to previous work, we extend the coupling model by a matching network as a method for partly compensating mutual coupling effects. We consider a multiport conjugate match designed for optimal decorrelation [10], [12]. To show the effects of mutual coupling in a massive MIMO system, the coupling model is applied to the 3GPP 3D channel model [13] that does not consider antenna coupling by itself.

II. Matrix Coupling Model

Mutual coupling of antennas means that the electromagnetic field produced by one antenna alters the current distribution of another antenna. Although this simply means that there is transmission between these two antennas, which is also the case between an antenna at a base station and an antenna at a mobile, mutual coupling mainly refers to an unintended coupling between co-located antennas of a node. In free space, two antennas need to be placed infinitely far apart in order to be uncoupled. The amount of coupling is either described by means of scattering parameters or impedance parameters that are measured between the two coupled antennas.

Considering an antenna array at the base station of a mobile communications network, antenna elements are usually spaced in close proximity, typically less than a wavelength from each other, leading to significant coupling between them. For massive MIMO systems below 6 GHz, deploying compact arrays with element spacings lower than half a wavelength is necessary due to physical array dimensions. For example in [14] authors measure with a large array of 128 elements at 2.6 GHz; at half wavelength antenna spacing this array is 7.3 m long.

Mutual coupling of array elements leads to two effects. Firstly the array pattern is altered compared to the hypothetical uncoupled case. Secondly, since the excitation of one element alters the current of another element. The impedance of one antenna array port, which is referred to as scan impedance, then depends on the excitation of all antenna elements. Therefore a coupled array cannot be steered to any direction α as an impedance mismatch occurs. For example, a Uniform Linear Array (ULA) array that is matched to front-fire cannot be steered to end-fire [15].

ISBN 978-0-9928626-7-1

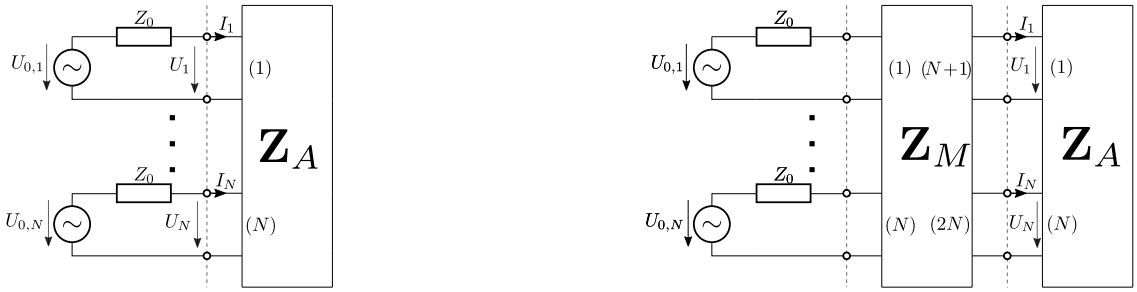

(a) Excitation $\mathbf{U}_0$ and coupled antenna array $\mathbf{Z}_\mathrm{A}$.

(b) Excitation $\mathbf{U}_0$, matching network $\mathbf{Z}_\mathrm{M}$ and coupled antenna array $\mathbf{Z}_\mathrm{A}$.

Fig. 1. Free excitation circuit models for transmission.

To reduce the amount of coupling between elements, that is, to increase inter-element isolation, the pattern of each element has to be modified such that the radiation is focused towards front-fire rather than in the direction of adjacent elements. This corresponds to usage of directive array elements as often suggested for millimeter wave communications [16]. Employing high gain antennas, however, also leads to a reduced angular steering range since the element pattern is then more directive in favor of front-fire and there is again no power towards end-fire possible. This limited steering range has an impact on the channel capacity when waves depart towards users with a high angular spread, as it is the case for Non Line Of Sight (NLOS) conditions. In this work, we assume dipole antenna elements that show a significant amount of mutual coupling. To compensate the impact on the channel capacity, we consider a matching network rather than shaping element patterns.

To include effects of mutual coupling in a channel model, we utilize the coupling matrix model from [17]–[19]. Below we derive the coupling matrix for the transmit case, while the derivation is similar for the receive case. The coupling model is then augmented in order to include effects of a matching network.

For derivation of the coupling model, we consider the circuitry shown in Fig. 1a. Source voltages described by $\mathbf{U}_0 = (U_{0,1}, \ldots, U_{0,N})^T$ for the antenna ports $n = \{1, \ldots, N\}$ together with reference impedances Z_0 model signal sources of constant available power. This is referred to as free excitation model since the antenna array port currents $\mathbf{I} = (I_1, \ldots, I_N)^T$ and the port voltages $\mathbf{U} = (U_1, \ldots, U_N)^T$ are not directly controllable but depend on source voltages as shown below.

The linear array is described by the impedance matrix $\mathbf{Z}_\mathrm{A} \in \mathbb{C}^{N \times N}$. We assume the antenna elements to be of minimum scattering type, that is, an element's input impedance is not influenced by the presence of other array elements [20]. Then the diagonal elements $\mathbf{Z}_\mathrm{A}[n, n]$ are given by the single element impedance in free space. We consider thin half-wavelength dipole antennas which fulfill this property. The off-diagonal elements $\mathbf{Z}_\mathrm{A}[n, m]$ for $n \neq m$ describe mutual coupling between the elements $n = \{1, \ldots, N\}$ and $m = \{1, \ldots, N\}$. For thin half-wavelength dipoles, there exist analytic solutions for self impedances and mutual impedances as a function of geometry [15], [21]. The array impedance matrix can be calculated as explained above for any minimum scattering antenna when mutual impedance information is available. In this case, the presented method is applicable to any array configuration.

The far-field of a dipole antenna is proportional to the feed current. For the free excitation model shown in Fig. 1a, the antenna feed current is described by

$$\mathbf{I} = \left(Z_0 \mathbf{E} + \mathbf{Z}_\mathrm{A}\right)^{-1} \mathbf{U}_0 \ , \tag{1}$$

where $\mathbf{E}$ denotes the identity matrix. The scan impedance of port n is defined as the port voltage to current ratio

$$Z_{s,n} = \frac{U_n}{I_n} \ , \tag{2}$$

when all ports are excited. The scan impedance is therefore different from the antenna element impedance $\mathbf{Z}_\mathrm{A}[n, n]$ at port n which is obtained only when all other ports are open circuited. Inserting the antenna array's voltage current relation $\mathbf{U} = \mathbf{Z}_\mathrm{A}\mathbf{I}$ into (2) we obtain

$$Z_{s,n} = \sum_{j=1}^{N} \mathbf{Z}_\mathrm{A}[n, j] \frac{\mathbf{I}[j]}{\mathbf{I}[n]} \ . \tag{3}$$

Note that the scan impedance of port n depends on the excitation of all ports. In the context of beamforming this corresponds to the fact that the amount of reflected and transmitted power depends on the beam angle α due to mutual coupling. When the antenna array is coupled, there exist beam directions where no power is radiated to or received from. Mutual coupling reduces the possible angular range for beamsteering. The scan reflection coefficient at antenna port n is defined as

$$\Gamma_n = \frac{Z_{s,n} - Z_0}{Z_{s,n} + Z_0} \ . \tag{4}$$

Please note that the scan reflection coefficient is different from the classical notion of a reflection coefficient. While the classical reflection coefficient of port n is defined for all other ports terminated with the respective reference impedance, the scan reflection coefficient at port n is obtained with all ports

ISBN 978-0-9928626-7-1 © EURASIP 2017

excited. Therefore, the scan reflection coefficient of any port n depends on the excitation (antenna current) of all antenna elements via (3).

A. Coupling Matrix

For equal antennas, when no coupling is present, all mutual impedances are zero and

$$\mathbf{Z}_{\mathrm{A}} = Z_{\mathrm{E}}\mathbf{E} \ , \tag{5}$$

with an arbitrary antenna element impedance Z_{E}. Inserting this in (1) yields the voltage to current relation for the uncoupled case

$$\mathbf{I} = \frac{1}{Z_0 + Z_{\mathrm{E}}}\mathbf{U}_0 \ . \tag{6}$$

We expand (1) by the factor found in (6) to obtain

$$\mathbf{I} = \underbrace{\frac{1}{Z_0 + Z_{\mathrm{E}}}\left(Z_0 + Z_{\mathrm{E}}\right)}_{=1}\left(Z_0\mathbf{E} + \mathbf{Z}_{\mathrm{A}}\right)^{-1}\mathbf{U}_0 \ , \tag{7}$$

from which the well-known coupling matrix is deduced to be

$$\mathbf{C} = \left(Z_0 + Z_{\mathrm{E}}\right)\left(Z_0\mathbf{E} + \mathbf{Z}_{\mathrm{A}}\right)^{-1} \ , \tag{8}$$

such that

$$\mathbf{I} = \frac{1}{Z_0 + Z_{\mathrm{E}}}\mathbf{C}\mathbf{U}_0 \ . \tag{9}$$

Due to the introduced normalization, we obtain a coupling matrix that evaluates to the identity matrix $\mathbf{E}$ in the hypothetical case of no coupling between antenna elements of impedance Z_{E}. This ensures applicability to any channel model by having no effect in the uncoupled case.

B. Multiport Conjugate Matching

We introduce a matching network $\mathbf{Z}_{\mathrm{M}} \in \mathbb{C}^{2N\times 2N}$ to the system as shown in Fig. 1b. Although the antenna array is described by impedance parameters, a matching network is commonly designed in scattering parameter description for convenience by

$$\mathbf{S}_{\mathrm{M}} = \begin{pmatrix} \mathbf{S}_{11} & \mathbf{S}_{12} \\ \mathbf{S}_{21} & \mathbf{S}_{22} \end{pmatrix} \ . \tag{10}$$

Several methods of matching a coupled antenna array are known [22]. By choosing $\mathbf{S}_{22} = \mathbf{S}_{\mathrm{A}}^{H}$ (the hermitian equivalent of $\mathbf{Z}_{\mathrm{A}}$), the power transfer is maximized for any choice of excitation. Thereby the scan reflection coefficient for the matched case is independent of the steering angle α. However, this only means that a perfect match is achieved for any excitation but does not mean that mutual coupling effects are completely compensated.

The design of a reciprocal and lossless matching network achieving a conjugate match does not lead to a unique solution. We choose the matching network known to have optimal decorrelation properties for symmetric dipoles [10]. For convenience, the matching network scattering parameter solution for (10) is provided in the appendix. The impedance parameter description is then obtained by transformation

$$\mathbf{Z}_{\mathrm{M}} = Z_0\left(\mathbf{E} - \mathbf{S}_{\mathrm{M}}\right)^{-1}\left(\mathbf{E} + \mathbf{S}_{\mathrm{M}}\right) \ , \tag{11}$$

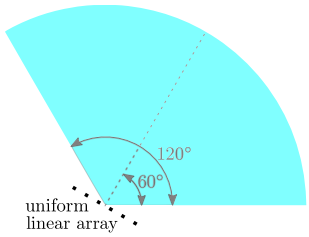

Fig. 2. Single sector network geometry. Users are uniformly distributed within one sector of 120°. A ULA is used at the base station.

and is partitioned in the blocks $\mathbf{Z}_{11}$, $\mathbf{Z}_{12}$, $\mathbf{Z}_{21}$ and $\mathbf{Z}_{22}$ analogously to (10).

Similar to (1), the excitation voltage $\mathbf{U}_0$ to antenna current $\mathbf{I}$ relation for the circuity shown in Fig. 1b is calculated to be

$$\mathbf{I} = \left(\mathbf{Z}_{\mathrm{A}} + \mathbf{Z}_{22}\right)^{-1}\mathbf{Z}_{21}\left(Z_0\mathbf{E} + \tilde{\mathbf{Z}}\right)^{-1}\mathbf{U}_0 \ , \tag{12}$$

with

$$\tilde{\mathbf{Z}} = \mathbf{Z}_{11} - \mathbf{Z}_{12}\left(\mathbf{Z}_{\mathrm{A}} + \mathbf{Z}_{22}\right)^{-1}\mathbf{Z}_{21} \ . \tag{13}$$

Similar to (8), we introduce a coupling matrix including a matching network

$$\mathbf{C} = c\left(\mathbf{Z}_{\mathrm{A}} + \mathbf{Z}_{22}\right)^{-1}\mathbf{Z}_{21}\left(Z_0\mathbf{E} + \tilde{\mathbf{Z}}\right)^{-1} \ , \tag{14}$$

where again the scalar $c \in \mathbb{C}$ in (14) is chosen such that $\mathbf{C} = \mathbf{E}$ for the hypothetical case of no coupling, that means for $\mathbf{Z}_{\mathrm{A}} = Z_{\mathrm{E}}\mathbf{E}$. The factor c therefore fulfills the same purpose as the factor $(Z_0 + Z_{\mathrm{E}})$ in (8) and has the physical dimension Ohm.

Let $\tilde{\mathbf{H}} \in \mathbb{C}^{M\times N}$ denote an uncoupled channel matrix consisting of channel coefficients from N transmit antennas to M receive antennas. The coefficients $\tilde{\mathbf{H}}$ describe a narrowband channel ignoring mutual coupling, i.e., a channel coefficient $\tilde{\mathbf{H}}[m,n]$ from transmit antenna n to receive antenna m is obtained in the absence of all other transmit and receive antennas. Mutual coupling effects at the transmit side antenna array are included in the coupled channel matrix

$$\mathbf{H} = \tilde{\mathbf{H}}\mathbf{C} \ . \tag{15}$$

By this, effects of mutual coupling are straight forward to include in any channel model once the array's impedance matrix $\mathbf{Z}_{\mathrm{A}}$ is known.

From (15) it is obvious that a simple zero-forcing receiver compensates effects of mutual coupling by inverting the coupling matrix [17]. In the context of mobile communications however, this leads to noise enhancement for small eigenvalues of $\mathbf{H}$.

III. Simulation Results

For simulations, channel coefficients are generated exploiting the 3GPP 3D channel model [13], [23]. We consider massive MIMO downlink transmissions in an urban macrocell scenario [13] with users uniformly distributed in a single sector ranging from 0 to 120° as shown in Fig. 2. A ULA of 200 vertical dipoles is placed at the base station such that

ISBN 978-0-9928626-7-1

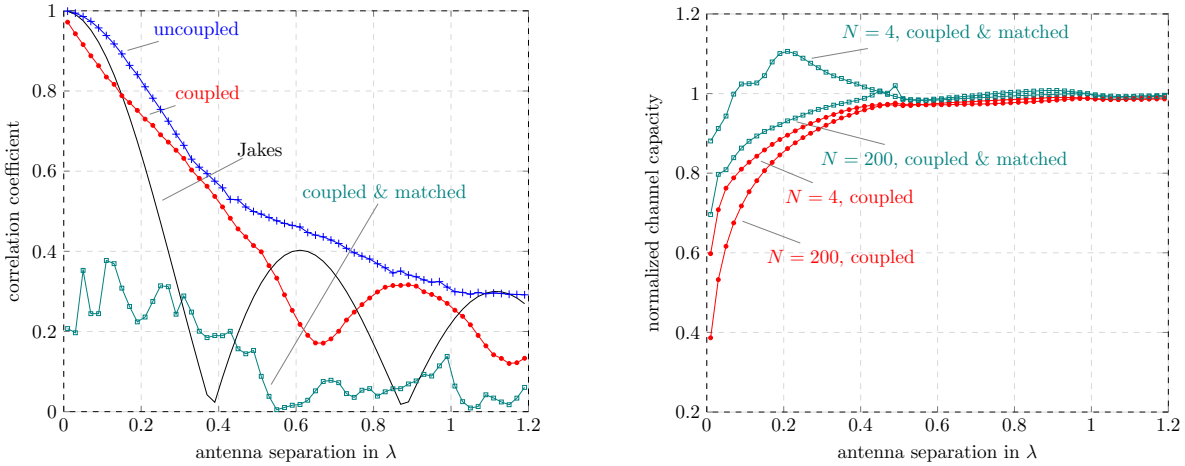

(a) Mean correlation coefficient absolute value for $N = 200$.

(b) Channel capacity normalized to the uncoupled case.

Fig. 3. Simulation results obtained with the 3GPP 3D channel model for a single user.

the broadside direction of 60° corresponds to front-fire. A user within the sector is assumed to be in NLOS and has one vertical dipole antenna. The element pattern for half-wavelength dipoles from [15] was implemented in the 3D channel model. Small scale channel coefficients from 200 antenna elements to a user with a single receive antenna were then generated exploiting the channel model. Next, the coupling matrix model was applied. Results were obtained by averaging over 10 000 channel realizations.

The magnitude of the average correlation coefficient for different antenna element spacings is shown in Fig. 3a. The correlation coefficient values for the *uncoupled* case are obtained from channel coefficients $\tilde{\mathbf{H}}$ generated by the 3D channel model that does not consider coupling effects. Values for the *coupled* and *coupled & matched* case are calculated including the coupling matrix via (15). For the former case, the coupling matrix is given by (8) while for latter case the matching network is included leading to the coupling matrix (14). The correlation coefficient obtained under the assumption of uniformly distributed Angles of Departure (AoD)s is plotted for comparison and labeled as *Jakes*.

Due to the distribution of users in a single cell and the resulting AoDs, uncoupled channel coefficients show a significant amount of correlation that decreases only slowly with antenna separation. When mutual coupling is included, correlation decreases faster with antenna separation even when no matching is included. Considering the coupled and matched case, the matching network is chosen to achieve a multiport conjugate match and ideal decorrelation, see [10], [12]. This solution is also provided in the appendix. While perfect decorrelation was obtained in [10] for two symmetric dipoles and AoD from all directions, the *coupled & matched* curve in Fig. 3a shows that low correlation is also obtained for 200 dipoles and a limited distribution of AoDs.

For channel coefficients directly obtained from the 3GPP 3D channel model, uncoupled channel capacity is almost constant over antenna separation. For comparability, channel capacities shown in Fig. 3b are normalized to the uncoupled case. The Signal to Noise Ratio (SNR) is chosen to be 20 dB for $N = 4$ antennas when conjugate beamforming is applied. For the same total transmit power, an SNR of 37 dB is achieved with $N = 200$. When the mutual coupling model is included, a strong impact on capacity is visible for antenna spacings smaller than half a wavelength. For small antenna spacings, not only does the mutual impedance between dipoles increase, but also more elements are within close proximity of each other, contributing significantly to the mutual coupling. Therefore, capacity decreases faster with decreasing antenna distance for $N = 200$ compared to $N = 4$. For element spacings larger than half-wavelength, effects of coupling on the capacity become negligible for dipole antennas in a ULA configuration. For other array geometries, with more than two nearest neighboring elements, like in a rectangular planar array, effects of coupling will be more severe.

When a multiport conjugate matching network is introduced, correlation is decreased and channel capacity is increased significantly for narrow spacings, compared to the unmatched case. Without any matching, a significant amount of transmit power is lost due to reflection for certain excitations. The power transfer to the antenna array is maximized for any choice of excitation by the conjugate matching network. Still, matching cannot reduce the mutual coupling of the antenna array, that is, $\mathbf{Z}_\mathrm{A}$ is unchanged, and certain beam patterns cannot be formed by the coupled array. With a high number of $N = 200$ antennas, relative capacity gains between the unmatched and matched case are smaller compared to a low number of $N = 4$ antennas. Although matching is less effective for high numbers of antennas and its implementation is not straight forward in practice, matching is a mutual coupling compensation method to consider for compact arrays.

IV. Conclusion

We introduced a universal coupling matrix model including a matching network, which is straight forward to include in any

ISBN 978-0-9928626-7-1 © EURASIP 2017

channel model. We applied this model to the 3GPP 3D channel model to obtain simulation results exploiting a standardized MIMO channel model. The 3D channel model considers clusters of scatterers between the users and the base stations. The AoDs are generated randomly following a wrapped Gaussian distribution. Channel coefficients show high correlation, which is slowly decreasing with antenna distance. We showed that the matching network choice for perfect decorrelation also works for large arrays and a channel with initially high correlation. Further, results show that mutual coupling has a stronger impact when the number of antennas increases, since mutual impedance between antennas decreases slowly with distance. Therefore, not only nearest neighboring elements need to be considered in the context of mutual coupling. We conclude that channel capacity loss due to mutual coupling can partly be compensated by a multiport conjugate matching network. However, for a large array, the implementation of a matching is practically challenging.

APPENDIX A
MULTIPORT CONJUGATE MATCH

For convenience, the matching network derivation is given in scattering parameter description. The antenna array's S-parameter matrix is obtained by transformation

$$\mathbf{S}_{\mathrm{A}} = \left(\mathbf{Z}_{\mathrm{A}} - Z_0\mathbf{E}\right)\left(\mathbf{Z}_{\mathrm{A}} + Z_0\mathbf{E}\right)^{-1} \ . \tag{16}$$

Let $\mathbf{S}_{\mathrm{A}}^H = \mathbf{U}_{22}\mathbf{\Sigma}_{22}\mathbf{V}_{22}^H$ denote the singular value decomposition of $\mathbf{S}_{\mathrm{A}}^H$, such that $\mathbf{U}_{22} = \mathbf{V}_{22}^\star$ where $(\cdot)^\star$ denotes the complex conjugation. The matching network is designed to be lossless and reciprocal, therefore, $\mathbf{S}_{\mathrm{M}}^H\mathbf{S}_{\mathrm{M}} = \mathbf{E}$ and $\mathbf{S}_{\mathrm{M}}^T = \mathbf{S}_{\mathrm{M}}$ where $(\cdot)^H$ denotes the conjugate transpose. To achieve a multiport conjugate match [10], [12] the matching network is defined by

$$\mathbf{S}_{22} = \mathbf{U}_{22}\mathbf{\Sigma}_{22}\mathbf{V}_{22}^H \ , \tag{17a}$$

$$\mathbf{S}_{12} = i\mathbf{U}_{11}\mathbf{D}\left(\mathbf{E} - \mathbf{\Sigma}^2\right)^{1/2}\mathbf{V}_{22}^H \ , \tag{17b}$$

$$\mathbf{S}_{21} = -i\mathbf{U}_{22}\mathbf{D}^H\left(\mathbf{E} - \mathbf{\Sigma}^2\right)^{1/2}\mathbf{V}_{11}^H \ , \tag{17c}$$

$$\mathbf{S}_{11} = \mathbf{U}_{11}\mathbf{\Sigma}_{22}\mathbf{V}_{11}^H \ , \tag{17d}$$

with the diagonal phase shift matrix $\mathbf{D}$ of unit magnitude and unitary matrices $\mathbf{U}_{11}$ and $\mathbf{V}_{11}$. According to [10], [12] these quantities are chosen as $\mathbf{D} = i\mathbf{E}$, $\mathbf{U}_{11} = \mathbf{E}$ and $\mathbf{V}_{11} = \mathbf{U}_{11}^\star$ for perfect decorrelation.

ACKNOWLEDGMENT

The financial support by the Austrian Federal Ministry of Science, Research and Economy, the National Foundation for Research, Technology and Development, and by TU Wien is gratefully acknowledged. This work has been co-financed by A1 Telekom Austria AG and Nokia Solutions and Networks. The research has been co-financed by the Czech Science Foundation, Project No. 17-18675S "Future transceiver techniques for the society in motion," and by the Czech Ministry of Education in the frame of the National Sustainability Program under grant LO1401.

REFERENCES

[1] S. Schwarz and M. Rupp, "Society in motion: Challenges for LTE and beyond mobile communications," *IEEE Communications Magazine, Feature Topic: LTE Evolution*, vol. 54, no. 5, pp. 76–83, 2016.

[2] F. Rusek, D. Persson, B. K. Lau, E. G. Larsson, T. L. Marzetta, O. Edfors, and F. Tufvesson, "Scaling up MIMO: Opportunities and challenges with very large arrays," *IEEE Signal Processing Magazine*, vol. 30, no. 1, pp. 40–60, 2013.

[3] E. G. Larsson, O. Edfors, F. Tufvesson, and T. L. Marzetta, "Massive MIMO for next generation wireless systems," *IEEE Communications Magazine*, vol. 52, no. 2, pp. 186–195, 2014.

[4] L. Lu, G. Y. Li, A. L. Swindlehurst, A. Ashikhmin, and R. Zhang, "An overview of massive MIMO: Benefits and challenges," *IEEE Journal of Selected Topics in Signal Processing*, vol. 8, no. 5, pp. 742–758, 2014.

[5] T. L. Marzetta, "Noncooperative cellular wireless with unlimited numbers of base station antennas," *IEEE Transactions on Wireless Communications*, vol. 9, no. 11, pp. 3590–3600, 2010.

[6] S. Schwarz and M. Rupp, "Limited feedback based double-sided full-dimension MIMO for mobile backhauling," in *50th Asilomar Conference on Signals Systems and Computers*, Asilomar, CA, 2016.

[7] J. Vieira, F. Rusek, and F. Tufvesson, "Reciprocity calibration methods for massive MIMO based on antenna coupling," in *IEEE Global Communications Conference (GLOBECOM)*. IEEE, 2014, pp. 3708–3712.

[8] C. Shepard, H. Yu, N. Anand, E. Li, T. Marzetta, R. Yang, and L. Zhong, "Argos: Practical many-antenna base stations," in *Proceedings of the 18th annual international conference on Mobile computing and networking*. ACM, 2012, pp. 53–64.

[9] E. Björnson, J. Hoydis, M. Kountouris, and M. Debbah, "Massive MIMO systems with non-ideal hardware: Energy efficiency, estimation, and capacity limits," *IEEE Transactions on Information Theory*, vol. 60, no. 11, pp. 7112–7139, 2014.

[10] J. W. Wallace and M. A. Jensen, "Mutual coupling in MIMO wireless systems: a rigorous network theory analysis," *IEEE Transactions on Wireless Communications*, vol. 3, no. 4, pp. 1317–1325, Jul. 2004.

[11] P.-S. Kildal and K. Rosengren, "Correlation and capacity of mimo systems and mutual coupling, radiation efficiency, and diversity gain of their antennas: simulations and measurements in a reverberation chamber," *IEEE Communications Magazine*, vol. 42, no. 12, pp. 104–112, 2004.

[12] J. W. Wallace and M. A. Jensen, "Termination-dependent diversity performance of coupled antennas: Network theory analysis," *IEEE Transactions on Antennas and Propagation*, vol. 52, no. 1, pp. 98–105, 2004.

[13] 3rd Generation Partnership Project (3GPP), "Study on 3D channel model for LTE," 3rd Generation Partnership Project (3GPP), TR 36.873, Jun. 2015.

[14] S. Payami and F. Tufvesson, "Channel measurements and analysis for very large array systems at 2.6 GHz," in *6th European Conference on Antennas and Propagation (EUCAP)*. IEEE, 2012, pp. 433–437.

[15] C. A. Balanis, *Antenna Theory: Analysis and Design*. John Wiley & Sons, 2005.

[16] E. Zöchmann, M. Lerch, S. Caban, R. Langwieser, C. Mecklenbräuker, and M. Rupp, "Directional evaluation of receive power, rician k-factor and rms delay spread obtained from power measurements of 60 ghz indoor channels," in *Topical Conference on Antennas and Propagation in Wireless Communications*. IEEE, 2016, pp. 246–249.

[17] H. Steyskal and J. S. Herd, "Mutual coupling compensation in small array antennas," *IEEE Transactions on Antennas and Propagation*, vol. 38, no. 12, pp. 1971–1975, 1990.

[18] T. Svantesson, "The effects of mutual coupling using a linear array of thin dipoles of finite length," in *Proceedings., Ninth IEEE SP Workshop on Statistical Signal and Array Processing*. IEEE, 1998, pp. 232–235.

[19] B. Clerckx, C. Craeye, D. Vanhoenacker-Janvier, and C. Oestges, "Impact of antenna coupling on 2×2 MIMO communications," *IEEE Trans. on Vehicular Technology*, vol. 56, no. 3, pp. 1009–1018, 2007.

[20] A. J. Roscoe and R. A. Perrott, "Large finite array analysis using infinite array data," *IEEE Transactions on Antennas and Propagation*, vol. 42, no. 7, pp. 983–992, 1994.

[21] R. C. Hansen, *Phased Array Antennas*. John Wiley & Sons, 2009.

[22] B. K. Lau, J. B. Andersen, G. Kristensson, and A. F. Molisch, "Impact of matching network on bandwidth of compact antenna arrays," *IEEE Transactions on Antennas and Propagation*, vol. 54, no. 11, pp. 3225–3238, Nov. 2006.

[23] F. Ademaj, M. Taranetz, and M. Rupp, "3GPP 3D MIMO channel model: A holistic implementation guideline for open source simulation tools," *EURASIP Journal on Wireless Communications and Networking*, vol. 2016, no. 1, p. 55, 2016. [Online]. Available: http://dx.doi.org/10.1186/s13638-016-0549-9